New improvements in the characterization of refractory gold in pyrites: An electron microprobe, Mössbauer spectrometry and ion microprobe study

P.Marion
INPL-ENS. Géologie Nancy, CRVM, Vandoeuvre les Nancy, France

P.Holliger
CEA-CEN & CEREM, Grenoble, France

M.C.Boiron & M.Cathelineau
GS CNRS-CREGU, Vandoeuvre les Nancy, France

F.E.Wagner
Physik Department, Technische Universität München, Garching bei München, Germany

ABSTRACT: Studies of pyrites by Mössbauer spectroscopy have shown the presence of gold in a combined state probably inserted within the lattice. In order to enhance detection limits for in-situ quantitative gold analyses, new SIMS investigations have been made thanks to a Resistive Anode Encorder record of the ion emissions, which provides digital images or scans of any part of the analyzed volume. Quantitative analysis of gold have been carried out thanks to 2 MeV ion implantation of gold in reference sulfide crystals, and the bulk composition of a pyrite grain has been determined. Some strong enrichments in gold and arsenic at the crystal margin attest fluctuations in the fluid chemistry and may be interpreted as a final growth zone, which is similar to that observed on arsenopyrite crystals. This multidisciplinary approach constitutes a powerful tool for the investigation of the insertion and distribution of trace elements within crystals, especially gold in sulfides at low contents down to a few ppm.

INTRODUCTION

The occurrence of tiny gold particles disseminated within massive pyrite veins are, in some instances, interpreted as resulting from a gold release from the sulfide lattice, during microfracturing and recrystallization stages posterior to the early sulfide crystallization. Such a process is considered as a prerequisite for significant gold enrichment from the previous disseminated ores. Thus, the study of auriferous ores free of visible native gold is of great interest for the knowledge of the process at the origin of a possible gold release and reconcentration. Such study has also been encouraged by a renewal in the recent years of the mining of deposits where gold is mostly borne by sulfides.

Paragenesis, crystal-chemistry and genesis of low grade Au-bearing sulfides are relatively poorly documented in comparison to the increasing data concerning the native Au bearing ores. Such a situation comes partly from the difficulty of gold analysis and mapping at low concentrations.

Run of mine gold ores usually contain a few ppm of gold whereas gravity or flotation concentrates may contain several hundred or thousand ppm. Even for these last high values, mineralogical methods such as microscopic examination or X ray diffraction remain inadequate to determine whether the gold is present as "native" metallic particles, or as other well defined gold minerals (such as tellurides), or even as substituted trace atoms in the structure of host minerals (such as arsenopyrite (see Cabri et al. 1989) and pyrite). Scanning electron microscopic examination is even often unsuccessfull whereas gold contents in sulfide host minerals are rarely high enough to exceed the detection limits of the electron microprobe analyser. All these facts have direct consequences on extractive metallurgy processes as well as on previous geological estimations. For example, the lock-up of gold within arsenopyrite or pyrite forbids direct cyanidation and necessitates a full conversion of the host mineral by oxidative processes (such as thermal "roasting", or chemical or bacterial oxidation). These treatments limit the feasability of projects concerning small ore bodies. It is clear that the exploration and ore beneficiation need in that case a close mineralogical control of the state, location and distribution of gold in the ores.

Thus, this paper presents multidisciplinary studies of pyrite samples, focused on the analytical problem of gold chemical state, location, mapping and analysis within crystals at low concentration.

1 PRELIMINARY ANALYSIS BY SEM AND ELECTRON MICROPROBE

Pyrites have been examined by scanning electron microscopy (S.E.M.) using secondary electron as well as back-scattered electron modes, which reveals very small differences around 0.1 in the distribution of the average atomic nunber (Z). Systematic quantitative electron microprobe (Q.E.M.) analyses were performed on a SX Cameca apparatus (Nancy University), using the following analytical conditions: accelerating voltage : 30 kV, 50 nA, counting time : 200 s, background for Au Lα calculated with a carefully determined slope. The

detection limit for gold in pyrite is 400 ppm under these analytical conditions at probability levels of 95%. Fe, As, S and Sb were analyzed together with gold. The detection limits were 460 and 160 ppm for As and Sb.

S.E.M. microphographs in the backscattered electron mode show that crystals exhibit complex and various chemical zonings due to variations essentially of the As/S ratio. These microphotographs reveal chemical changes in the crystals from one growth zone to another (as described by Fleet et al., 1989). Figures 2, 3, 5 and 6 show some of these As-enriched pyrite grains, all from auriferous mineral associations. In one of the photographied grains, "visible" metallic gold is present (figure 3).

Q.E.M. analysis fails very often to reveal any concentration of gold within pyrite (i.e. above the detection limit), excepted in certain particular paragenesis such as those encountered in the Villeranges deposit, France (Boiron et al. 1989) (figure 6 and the corresponding explanatory drawing of figure 7), or in a Columbian deposit (figures 2 and 3).

When detectable, the Au content may be positively related to the As content (fig.1, corresponding to pyrites of the Villeranges deposit, see fig.6), as in the case of arsenopyrites (Cathelineau et al. 1989), but the low gold levels make difficult any further interpretation.

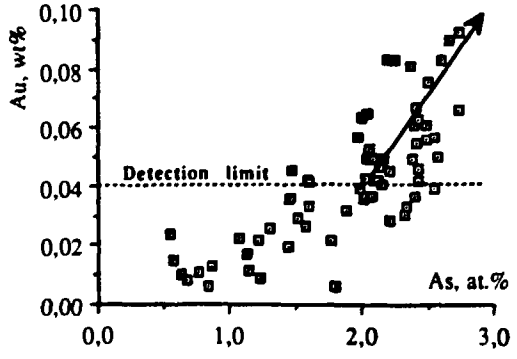

Figure 1. Au-As plot (QEM analyses) for some pyrites from the Villeranges prospect, same ore and type as that presented on figures 6 and 7. The linear trend drawn through the points above the detection limit is only indicative.

Arsenic and sulfur are negatively correlated, but the significance of this observation remains speculative, since diluted As in the pyrite lattice or crypto-inclusions of arsenopyrite may give the same As-S relationship when analyzed by QEM (as for exemple the analyses on the pyrite of figure 5).

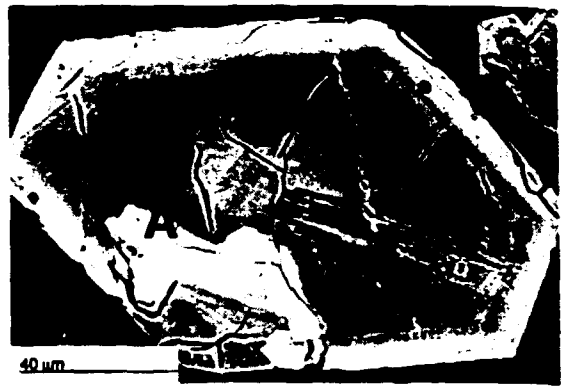

Figure 2. Backscattered electrons SEM image of a pyrite crystal from a Columbian deposit. The rim enriched in As is complicated by a colloform-type structure (white zone A), characterized by high concentrations of gold (up to 3,000 ppm) and arsenic (up to 7%).

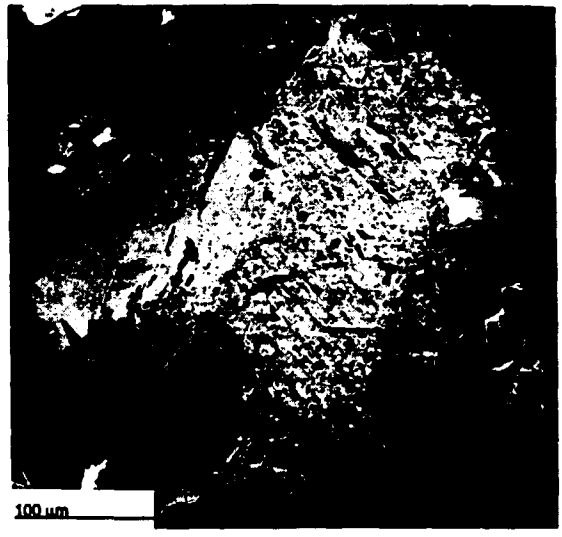

Figure 3. Backscattered electrons SEM image of a pyrite crystal from the same Columbian deposit. Heterogeneous parts of the grain are characterized by an increased porosity and the presence of inclusions of metallic gold (A). The homogeneous part of the grain shows local brighter zones (increased av. Z number) (B), where high concentrations of arsenic and gold are present.

2 ^{197}AU MÖSSBAUER SPECTROSCOPY

^{197}Au Mössbauer spectroscopy has proven to be a powerful tool for the characterization of the mineralogical and chemical state of gold in ores, mineral concentrates or metallurgical products (Marion *et al.*, 1986, 1988a and b).

In many ores or concentrates containing arsenopyrite, significant amounts of gold are identified to be at a combined state. A replacement of

iron by gold in the lattice of arsenopyrite (Johan *et al.*, 1989, Cathelineau *et al.*, 1989) is assumed in that case. In these cases, the relative amounts of chemically bound gold and metallic gold can be calculated and used for the prediction of metal recoveries by direct cyanidation (Wagner *et al.*, 1989).

Figure 4 shows a spectrum recorded on a pyrite concentrate from Columbia: the chemically combined gold predominates, whereas a small shoulder peak indicates the presence of metallic gold (figure 3). The large absorption peak corresponding to the combined form of gold is shifted towards negative values of velocity in comparison with the well-known position of gold combined within arsenopyrite. This indicates clearly that, in this sample, the gold is not chemically locked-up within inclusions of arsenopyrite in pyrite, although it occurs frequently in other ores (figure 5). This spectrum gave the first explanation for the bad recoveries encountered during the direct cyanidation of the ore. Taking into account the element distribution given by SEM backscattered electron images (figures 2 and 3), further QEM studies on the pyrite concentrate produced from cyanidized residues confirmed the presence of pyrite grains enriched in gold (up to 3,000 ppm) and in arsenic (up to 7%). This is the first evidence of combined gold within pyrite.

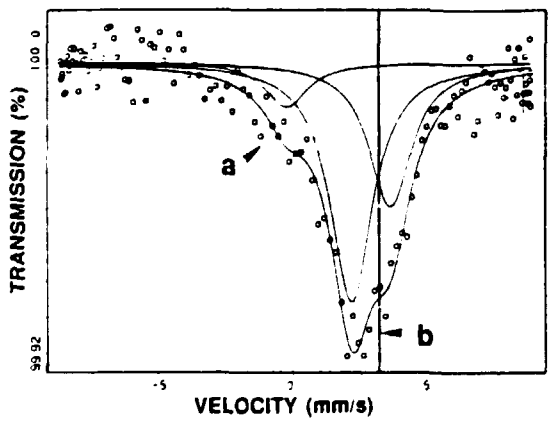

Figure 4. ^{197}Au Mössbauer spectrum of a pyrite concentrate (90 ppm Au) containing both metallic gold (a), and combined gold within pyrite (sample corresponding to the minerals presented on figures 2 and 3). Line (b) shows the centershift of the absorption peak of gold combined within arsenopyrite, which is more positive. The large peak of combined gold within pyrite is deconvoluted as two single peaks, which are one of the best fits for the experimental data, but whose physical significance remains unknown.

This form of gold is probably more frequent than currently described, but was missed because the average "invisible" gold contents in pyrites are lower than in arsenopyrites. It is, however, impossible to say in what form gold is bound within pyrite (interstitial atoms, substitution of iron, or even

Figure 5. Backscattered electrons SEM image of a pyrite crystal from Le Châtelet mine (France). Auriferous arsenopyrite crystals (A) along cracks, and slightly As-enriched zones (B) within the pyrite are visible.

crypto-inclusions of a gold-rich phase), unless other analytical tools are used.

2.1 Quantitative estimations

Quantitative calculations of the relative amounts of metallic and combined forms of gold have been successfully made on arsenopyrite concentrates: for this purpose, it is necessary to measure the relative areas of the absorption peaks of metallic and combined gold on the spectra, and to know the value of the Lamb-Mössbauer factor, which varies for each gold compound. This corrective factor has been estimated for gold combined to arsenopyrite (Wagner *et al.*, 1989) to be approximately 1.5, relative to pure metallic gold. Thus, the combined gold relative amount can be derived from the following formula:

FeAsS Combined Gold (%) =

$100/[1+(1.5*RA_{Au}/RA_{Comb.Au})]$

(where RA is the relative area).

The discovery of pyrites enriched in combined gold at high concentration levels (Mössbauer spectrum of figure 4, figures 2 and 3), gave the opportunity to establish a similar relation:

FeS_2 Combined Gold (%) =

$100/[1+(2.4*RA_{Au}/RA_{Comb.Au})]$,

where the Lamb-Mössbauer factor, 2.4, is considerably higher than for arsenopyrite, which a-posteriori confirms that the gold is not present in these pyrites as arsenopyrite inclusions. In this particular case, this determination has allowed the explanation of the bad recoveries of gold after cyanidation (max. 25%, which is very close from the calculated amount of metallic gold, which is 22%). Unfortunately, it is actually impossible to know whether the calculated factor should be used for other auriferous pyrites until new different samples are found and their Mössbauer spectra recorded.

3 SIMS STUDIES

3.1 Experimental procedure

The SIMS studies were carried out on a CAMECA IMS 3f recently equipped with a resistive anode encorder (RAE) elaborated by Charles Evans & Associates. Some changes in the operating conditions previously described (Cathelineau et al, 1989) have been made to enhance the accuracy of both digital images and ion measurements using the electron multiplier. A 10 keV Cs^+ primary ion beam (10-50 nA) was used and 14.5 keV negative secondary ions were detected. Measurements were acquired with no voltage offset at a mass resolution of 2000. This resolving power is enough for eliminating the molecular interferences $^{197}FeAsS_2^-$ and $^{197}CsS_2^-$ on ^{197}Au in gold bearing sulphides analysis (Marion, 1988,1989). The matrix ion intensities were monitored on the isotope $^{90}FeS^-$ for pyrite and on $^{90}FeS^-$ and $^{109}AsS^-$ for arsenopyrite.

3.2 Imaging using RAE

The RAE secondary ion detector is a device incorporated into the Cameca IMS 3f as a separate detector which uses microchannel plates to convert ions into a pulse of 10^6 electrons which the impact the resistive surface of an anode. It acts just as an electron multiplier ; however its deadtime of 3 µs limits the instantaneous countrate to 3.10^4 cts/s. It is a position sensitive detector which generates (x,y) coordinate for each detected ion: it allows digital images to be stored rapidly without intermediate steps in the RAE directory of the hard disk. Afterwards coordinates can be selected to define areas or line scans; this option constructs and displays a plot of ion intensity versus distance based on the define line coordinates and its width (in pixels). A pixel (the image unit) is equal to an elemental square of 0,6 and 1,5 µm side for images representing analyzed areas of 150 µm and 400 µm respectively. The software allows images to be displayed on the photographic reproduction with both logarithmic and linear pseudo-color versus intensity scales.

3.3 Gold implant and quantification

Ion implantation seems the best way to obtain quantitative elemental SIMS measurements in ore minerals. Concerning gold concentration in common sulphides, Chryssoulis et al. (1989), Cook and Chryssoulis (1990) developed calibrations of the ion microprobe using internal and external standards. In the internal standardization, a known amount of gold is implanted into the matrix to be analyzed. In the external standardization, selected standard or synthetic minerals are used to produce a specific calibration curve on the ion microprobe, depending on the mineral, the relative ion yields of gold and matrix ions, and the operating conditions. Data obtained from unknown samples are then compared with the calibration curves to determine gold concentrations. This method has been prefered for this study. It is faster, non "destructive" for the samples (i.e. no gold is added), less dependent of the mineral structures (micro-faults, inclusions, holes, along which gold may diffuse during the implantation) and permits the direct analysis of samples without a preleminary recording of the gold implant profile as internal standardization. However, the precision is highly dependent on the differences in the compositions of the standard and the analyzed mineral, which must match as closely as possible . In our pyrite samples, the concentrations vary within the global chemical formula $FeAs_xS_{1-x}$, which could induce for example a difference in the iron atomic concentration of app. 2% maximum between the standard and the analyzed zone of the sample, or between two areas of the sample.

The implant of gold was done at 2MeV and with a dose of $1.09.10^{15}$ at/cm^3 on natural minerals by the Ion Beam Services laboratory. These minerals were polished sections of monocrystals (area of app. 25 mm^2), which revealed to be optically perfect under the microscope and homogeneous under SEM and QEM analysis. The retained dose was controlled by Rutherford Backscattering Spectroscopy (RBS) analysis of an implanted Si wafer with an accuracy of 5 %.

The Relative Sensitivity Factors (RSFs) used to apply quantitative scales to SIMS data, can be easily calculated from the ion implant SIMS depth profile, by the following equation :

$$\text{Dose} = (RSF/I_m) \cdot \Sigma_i\, c(Z_i)$$

where I_m is the matrix isotope intensity in cts/s and $c(Z_i)$ the concentration of gold (at/cm^3) at the depth Z_i.

For pyrite, the molecular ion $^{90}FeS^-$ (^{56}Fe with the minor isotope ^{34}S of sulphur) presents a good and stable emission (see the ^{88}FeS emission on the scan of figure 9), which results from the quasi-constant concentration of iron in pyrite (see the aforementioned remark). The ^{90}FeS emission can be thus chosen as matrix isotope. On the implantation profile of gold in the pyrite standard, the maximum of the Au distribution is $2.93.10^{19}$ at/cm^3 at a depth of 2570 Å, as calculated by a computer simulation. Thus, taking into account the average density of FeS_2 ($2.51.10^{22}$ at/cm^3), the gold concentration at this depth is 1055 ppm atomic or 5200 ppm weight (ppmw). RSF can be then expressed relatively to the matrix isotope ^{90}FeS emission of the standard: RSF value for gold in pyrite is 12210 ppmw with respect to ^{90}FeS. Similar calculations have been made for other sulfide minerals. For pyrite samples of unknown composition, the absolute concentration of gold will be easily calculated in ppmw from the measured ion intensities, by the expression $RSF*(I_{^{197}Au}/I_{^{90}FeS})$.

The ion microprobe with RAE digital imaging equipment provides informations that may be directly

used for quantitative determination of the accumulation of trace elements in minerals or in parts of these minerals. The following calculation of the concentrations of gold in pyrite when this mineral is diluted in a much higher amount of auriferous arsenopyrite (i.e. impossible to separate without pollution), is a good example of the feasability of this technique.

3.4 Au-zoning in pyrite

The study was carried out on a polished section of a rich mineralized zone of the Villeranges orebody (France).

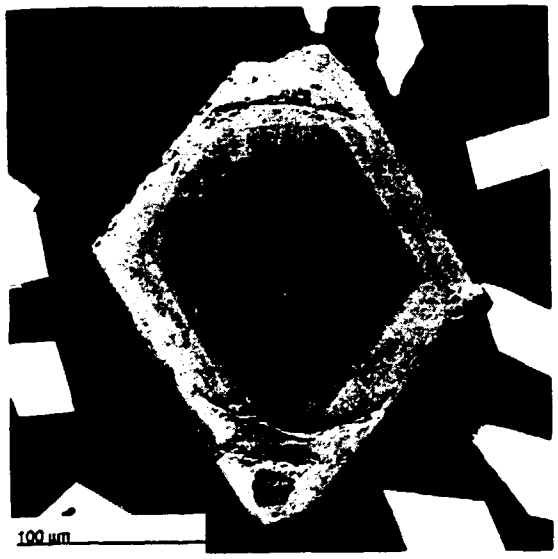

Figure 6. Backscattered electrons SEM image of a pyrite crystal from the Villeranges orebody (France). The bright zone is related with a higher As enrichment.

The microscopic examination shows large pyrite crystals strongly zoned for arsenic (Figure 6) and arsenopyrites exhibiting high gold contents (up to 0.8%, as measured by QEM analysis) in relation with zonal As enrichment. A sufficient weight of pure pyrite was impossible to concentrate for chemical analysis, due to a very high arsenopyrite/pyrite ratio.

The pyrite contains low concentrations of gold, as revealed by the electron microprobe with a long counting time : these concentrations are shown on figure 7, and are lower than 1000 ppm, which renders any Au Lα XRF mapping impossible.The external enrichment of gold within the pyrite crystal seems however to be similar to the patterns described for arsenopyrites in the same orebody and in others (Marion 1988, Cathelineau et al. 1989, Johan et al. 1989), which a similar Au-As relationship (figure 1).

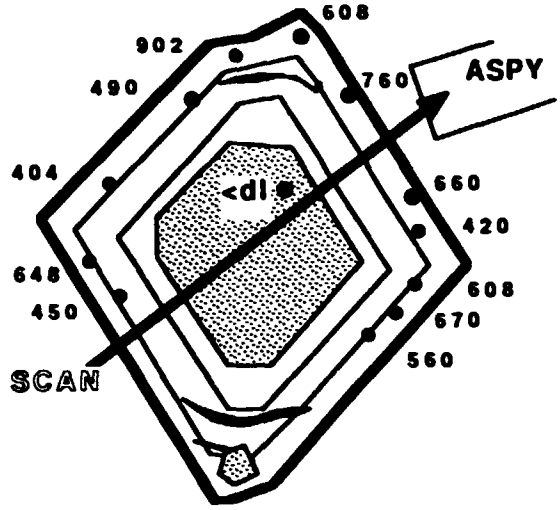

Figure 7. Schematic presentation of the pyrite shown on figure 1. The black dots correspond to electron microprobe analyses, with the determinated gold amount (ppm). The line accross the grain gives the direction of the ion microprobe scans represented on figures 9 and 10. This line cuts a part of an arsenopyrite grain in the top-right corner of the drawing.

The ion microprobe was therefore used to characterize the gold repartition in these pyrite crystals. Figure 8 presents the digital image obtained by monitoring the ^{197}Au emission on the grain of figures 6 and 7.

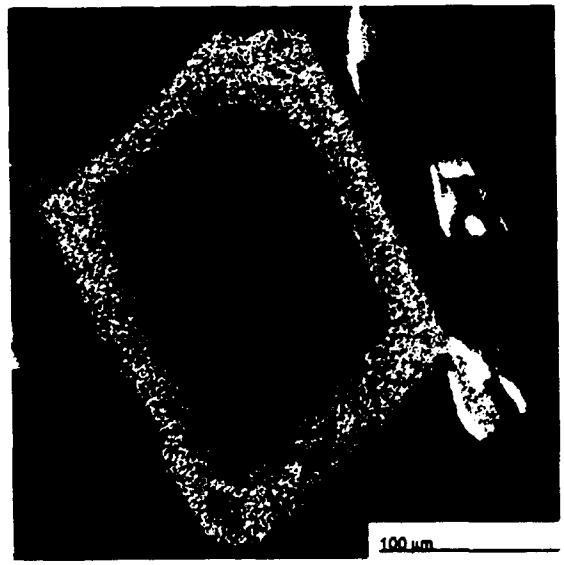

Figure 8. Digital mapping of the $^{197}Au^-$ ion secondary emission induced by a Cs^+ ion microprobe (raster 250µm) of the same pyrite crystal as on figure 6 and 7. Analytical conditions are given in the text.

The raw data for a line scan accross the grain (see scan position on figure 7) are given on figure 9: FeS^- and SbS^- emissions are constant, whereas AsS^- and Au^- emissions correspond to the observations by QEM, with an enriched zone around the grain: the correlation of figure 1 between the two elements As and Au is therefore confirmed. Antimony is relatively constant in pyrite, but probably at very low levels, as previously analyzed by QEM (content below the detection limit, i. e. <160 ppm). A small part of an arsenopyrite grain was analyzed together with pyrite: AsS, SbS and Au emissions are much higher than for pyrite, as expected after QEM analyses. One can notice that the negative correlation between Sb and Au in arsenopyrite (Marion 1988, Cathelineau et al. 1989, Johan et al. 1989) is not found for pyrite.

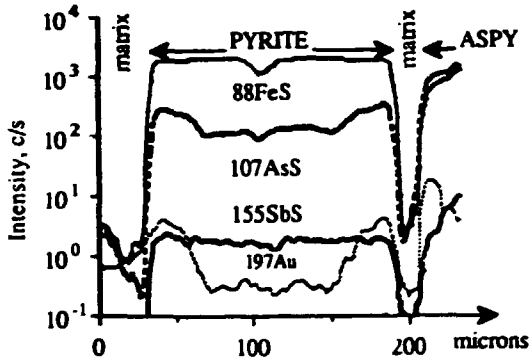

Figure 9. Ion microprobe scan accross the pyrite grain presented on figures 6 and 7. This scan is obtained from a digital image covering the whole grain (figure 8) and integ-rates a 20µm width band along the line of figure 7. A small part of an arsenopyrite grain is concerned by the right end of the scan. The depletions of FeS signal correspond to a hole (center of the pyrite) or to the silicate matrix.

The Au signal was then converted into concentration, and the new scan presented on figure 10.

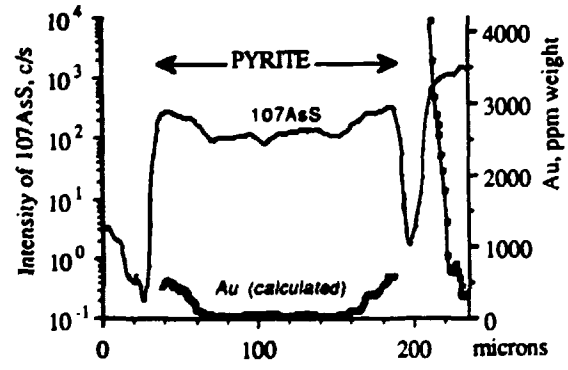

Figure 10. Calculated gold concentrations (ppm) along the scan (see figures 3 and 4). The RSFs used are 12210 ppmw for pyrite and 4820 ppmw for arsenopyrite with respect to ^{90}FeS. The concentrations in the silicate matrix are not calculated.

The maximum gold concentration in the pyrite is approximately 500-600 ppm in the enriched margin. This level is consistent with the values obtained with QEM (figure 7): this is a demonstration of the reliability of the quantification method. The calculated concentration within the arsenopyrite grain fits correctly QEM determinations too, and the peripheral enrichment in gold of the grain is clearly visible.

Assuming that the enriched margin of the pyrite grain has an average apparent thickness of 33µm, and that the grain is an octahedron (as revealed by SEM on separate pyrite crystals), it was calculated that the enriched margin volume represents 77,2% of the total. The average concentrations of the margin and of the core are obtained by integrating 20µm width bands accross the grain on digital images for ^{197}Au and ^{88}FeS emissions. The ^{197}Au to ^{90}FeS ratio is then calculated, and multiplicated by the RSF factor for gold in pyrite. Average concentrations are thus respectively 288 ppm Au in the margin and 44 ppm in the central zone. The approximative bulk concentration for the the grain is therefore 232 ppm, as directly derived from volume calculations. The enriched margin thus represents 95,7% of the included gold within this pyrite.

CONCLUSIONS

This study has shown that :

1. the quantification of the distribution of gold contents within crystals is now possible down to a few ppm using the S.I.M.S. technique. Improvements concern the quantification of the gold content through calibration using gold implanted standards, an enhanced sensitivity of the ion detection, and the mapping thanks to a RAE three dimen-sional digital record of the ion emission. The calculation of the bulk amount of gold in pyrite when this mineral is diluted in a much higher amount of auriferous arsenopyrite (i.e. impossible to separate without pollution), is a good example of application.

2. pyrites may bear, as arsenopyrites, a significant amount of combined gold, as revealed by ^{197}Au Mössbauer spectroscopy. This gold is probably inserted within the lattice, at levels reaching a few thousands ppm, in addition of the commonly observed inclusions of free gold particles.

3. the simultaneous characterization of major and trace element distribution within both pyrites and arsenopyrites provides valuable information on the evolution of the hydrothermal solution chemistry during the crystal growth. These minerals may be considered as precursors of later native gold particle enrichments. However, in studied quartz veins (Northern Massif Central (France), Morocco, ...), the gold peripheral enrichment of the crystals takes place during a relatively late and final stage of the metamorphic-hydrothermal processes. This seems to indicate that these minerals are not necessarily the precursors of further hydrothermal gold reconcentration.

4. One of the most effective process for the gold release is the leaching of its sulfide host minerals under supergene bio-chemical weathering. The combined-gold release from sulphides (in a complex ionic form or colloïdal reduced form) could be at the origin at less partially of the gold enrichment observed in gossans.

5. the multidisciplinay approach used in this study is of capital importance for any study of ores before, during or after dressing and beneficiation. It gives a quantification of the part of combined/metallic and refractory/leachable gold, as well as the part of gold born by the different kinds of minerals, and data on the distribution of gold within the minerals. These data are determining in technical or economical choices during feasability studies.

REFERENCES

Boiron, M.C., Cathelineau, M. and Trescases J.J. 1989. Conditions of gold bearing arsenopyrite crystallisation in the Villeranges basin, Marche-Combrailles shear zone, France: a mineralogical and fluid inclusion study. Economic Geology, 84: 1340-1362.

Cabri, L.J., Chryssoulis, S.L., De Villiers, J.P.R., Laflamme, J.H.G. and Buseck P.R. 1989. The nature of "invisible" gold in arsenopyrite. Canadian Mineralogist, 27: 353-362.

Cathelineau, M., Boiron, M.C., Holliger, P., Marion, P. and Denis, M. 1989. Gold-rich arsenopyrites : crystal-chemistry, gold location and state, physical and chemical conditons of crystallization. Economic Geology, Monograph 6 :"The Geology of Gold Deposits: The Perspective in 1988"; R. Keays, R. Ramsay, D. Groves edts.: 328-341.

Chryssoulis, S.L., Cabri, L.J. and Lennard, W. 1989. Calibration of the ion microprobe for quantitative trace precious metal analyses of ore minerals. Economic Geology, 84: 1684-1689.

Cook, N.J. and Chryssoulis, S.L. 1990. Concentrations of "invisible gold" in the common sulfides. Canadian Mineralogist, 28: 1-16.

Fleet, M.E., MacLean, P.J. and Barbier, J. 1989. Oscillatory-zoned As-bearing pyrite from strata-bound and stratiform gold deposits: an indicator of ore fluid evolution. Economic Geology, Monograph 6 :"The Geology of Gold Deposits: The Perspective in 1988"; R. Keays, R. Ramsay, D. Groves edts.: 356-362.

Johan, Z., Marcoux, E. and Bonnemaison, M. 1989. Arsénopyrite aurifère : mode de substitution de Au dans la structure de FeAsS. C.R. Acad. Sc. Paris, 308, II: 185-191.

Marion, P., Regnard, J.R. and Wagner, F.E. 1986. Etude de l'état chimique de l'or dans des sulfures aurifères par spectroscopie Mössbauer de ^{197}Au : premiers résultats. C.R. Acad. Sc. Paris, 302, II, 8: 571-574.

Marion, P., Wagner, F.E., Jumas, J.C. and Regnard, J.R. 1988. Apports de la spectroscopie Mössbauer à la con-naissance de l'état de liaison de l'or dans les sulfures. Proc. of the Conference "Gisements métallifères dans leur contexte géologique", (Johan Z. et Ohnenstetter D. ed.), Montpellier (oct. 1986). Doc. BRGM, 158: 509-525.

Marion P. 1988. Caractérisation de minerais sulfurés aurifères : mise en oeuvre de méthodes classiques et nouvelles. Thesis ès Sciences, INPL, Nancy.

Wagner, F.E., Marion, P. and Regnard J.R. 1988. ^{197}Au Mössbauer study of gold ores, mattes, roaster products and gold minerals. Hyperfine Interactions, 41: 851-854.

Wagner, F.E., Swash, P.M. and Marion, P. 1989. A ^{197}Au and ^{57}Fe Mössbauer study of the roasting of refractory gold ores. Hyperfine Interactions, 46: 681-688.